The future of cardiovascular magnetic resonance

All-in-one vs. real-time (Part 1)

Christodoulou, Anthony G.; Cruz, Gastao; Arami, Ayda; Weingärtner, Sebastian; Artico, Jessica; Peters, Dana; Seiberlich, Nicole

DOI
10.1016/j.jocmr.2024.100997

Publication date
2024

Document Version
Final published version

Published in
Journal of Cardiovascular Magnetic Resonance

Citation (APA)
Christodoulou, A. G., Cruz, G., Arami, A., Weingärtner, S., Artico, J., Peters, D., & Seiberlich, N. (2024). The future of cardiovascular magnetic resonance: All-in-one vs. real-time (Part 1). *Journal of Cardiovascular Magnetic Resonance*, *26*(1), Article 100997. https://doi.org/10.1016/j.jocmr.2024.100997

Journal of Cardiovascular Magnetic Resonance 26 (2024) 100997

Contents lists available at ScienceDirect

Journal of Cardiovascular Magnetic Resonance

journal homepage: www.sciencedirect.com/journal/jocmr

Review article

The future of cardiovascular magnetic resonance: All-in-one vs. real-time (Part 1)

Anthony G. Christodoulou[a,b], Gastao Cruz[c], Ayda Arami[d,e], Sebastian Weingärtner[d], Jessica Artico[f], Dana Peters[g], Nicole Seiberlich[c,*]

[a] Department of Radiological Sciences, David Geffen School of Medicine, University of California, Los Angeles, Los Angeles, CA, USA
[b] Biomedical Imaging Research Institute, Cedars-Sinai Medical Center, Los Angeles, CA, USA
[c] Michigan Institute for Imaging Technology and Translation, Department of Radiology, University of Michigan, Ann Arbor, MI, USA
[d] Department of Imaging Physics, Delft University of Technology, Delft, the Netherlands
[e] Department of Radiology, Leiden University Medical Center, Leiden, the Netherlands
[f] Barts Heart Centre, London, UK
[g] Radiology & Biomedical Imaging, Yale University, New Haven, CT, USA

ARTICLE INFO

Keywords:
Cardiac MRI
Rapid imaging
Real-time imaging
Quantitative imaging
Magnetic Resonance Fingerprinting
Multitasking
Parallel imaging
Compressed sensing

ABSTRACT

Cardiovascular magnetic resonance (CMR) protocols can be lengthy and complex, which has driven the research community to develop new technologies to make these protocols more efficient and patient-friendly. Two different approaches to improving CMR have been proposed, specifically "all-in-one" CMR, where several contrasts and/or motion states are acquired simultaneously, and "real-time" CMR, in which the examination is accelerated to avoid the need for breathholding and/or cardiac gating. The goal of this two-part manuscript is to describe these two different types of emerging rapid CMR. To this end, the vision of each is described, along with techniques which have been devised and tested along the pathway of clinical implementation. The pros and cons of the different methods are presented, and the remaining open needs of each are detailed. Part 1 will tackle the "all-in-one" approaches, and Part 2 the "real-time" approaches along with an overall summary of these emerging methods.

Introduction

The power of cardiovascular magnetic resonance (CMR) arises from its sensitivity to a uniquely wide range of physiological processes, image contrasts, and tissue states. This flexibility enables CMR to visualize anatomy, measure function and flow, and leverage physical processes such as nuclear magnetic resonance (NMR) relaxation to reveal tissue states including fibrosis and inflammation [1]. However, while CMR can be used to interrogate a large number of cardiac tissue/function features, each of these features is typically collected using a specific CMR pulse sequence [2]. For example, cine sequences are used to assess cardiac motion and function, contrast-enhanced perfusion scans for microvascular obstruction, late gadolinium for viability, T_1 mapping for infiltrative disease, T_2 mapping for edema, T_2* mapping for iron overload, etc. [3]. Most of these sequences must be performed during a breathhold to avoid artifacts due to respiratory motion, and many are gated such that data are collected only in a specific cardiac phase. Moreover, conventional CMR acquisitions collect 2D planes within the 3D structure of the heart, and thus several images must be collected if the whole heart is being evaluated; a common example of this is that 12–16 2D slices are collected in cine imaging to show the motion of the left ventricle from base to apex. In addition, the timing requirements of certain sequences can further complicate the CMR protocol. For example, extracellular volume fraction (ECV) mapping

Abbreviations: bSSFP, balanced steady-state free precession; CMR, cardiovascular magnetic resonance; CoV, coefficient of variance; ECG, electrocardiogram; ECV, extracellular volume fraction; EPI, echo-planar imaging; GRE, gradient echo; IR, inversion recovery; LGE, late gadolinium enhancement; MOLLI, modified Look-Locker inversion recovery; NMR, nuclear magnetic resonance; PDFF, proton density fat fraction; RF, radiofrequency; SNR, signal-to-noise ratio; SR, saturation recovery; T2, prepared; 2D, two-dimensional; 3D, three-dimensional; SASHA, saturation recovery single-shot acquisition; SAPPHIRE, saturation pulse prepared heart rate independent inversion-recovery sequence; QALAS, quantification using an interleaved Look-Locker acquisition sequence with a T2 preparation pulse; GraSE, gradient- and spin-echo; MRF, magnetic resonance fingerprinting; FLASH, fast low angle shot; DL, deep learning; AI, artificial intelligence; PACS, picture archiving and communication system; DICOM, diagnostic imaging and communications in medicine; RGB, red, green and blue; CMYK, cyan, magenta, yellow and key

* Corresponding author.
E-mail address: nse@med.umich.edu (N. Seiberlich).

https://doi.org/10.1016/j.jocmr.2024.100997
Received 21 December 2023; Accepted 10 January 2024

and late gadolinium enhancement (LGE) imaging require imaging at specific time points after the injection of contrast agent; the subsequent time spent waiting for the appropriate contrast to develop can also prolong exams.

As conventional CMR examinations require multiple images, each with a different contrast, in a different breathhold, over the entire 3D volume of the heart, CMR protocols can become quite long; many institutions plan 45–60 min per patient, and even these timeframes may be regularly exceeded in uncooperative patients or those with unusual anatomy. The expense and training required to successfully administer this long series of scans has made it difficult for CMR to grow beyond advanced academic medical centers. This limits its accessibility to large portions of the population in both high and low resource areas. Thus, there is an open need for rapid approaches for CMR acquisitions, both to reduce the acquisition time for individual images and sequences, and also to reduce the length of the overall protocol.

In recent years, several different schools of thought have emerged for reducing the length of CMR exams. One basic approach is to tailor the protocol specifically for a narrow clinical question, reducing the number of individual sequences that are used. As an example, a well-constructed 30-minute CMR exam [4] has been developed which can address a significant number of clinical indications. While this approach is used in many institutions, researchers are devising novel techniques to collect all contrasts in a more efficient manner. These techniques fall roughly into two categories: "all-in-one" approaches and "real-time" approaches. In the "all-in-one" approach (also referred to as SMART CMR [5]), novel sequences are designed to capture multiple forms of information simultaneously; in the most extreme case, motion fields and maps for tissue characterization could be acquired over the whole volume of the heart in a single comprehensive acquisition. In the "real-time" approach, each individual sequence is collected more rapidly, often fast enough to remove the need for breathholding and electrocardiogram (ECG) gating, thereby making the entire protocol much more efficient. Neither of these approaches has yet been fully deployed clinically due to associated technical challenges, but significant progress has been made towards portions of each type of novel protocol.

The goal of this two-part manuscript is to describe these two different types of emerging rapid CMR protocols, namely the "all-in-one" and the "real-time" approaches. To this end, the vision of each is described, along with techniques which have been devised and tested along the pathway of clinical implementation. The pros and cons of the different methods are presented, and the remaining open needs of each are detailed. Part 1 will tackle the "all-in-one" approaches, and Part 2 the "real-time" approaches along with an overall summary of these emerging methods.

"All-in-one" CMR

Vision of an "all-in-one" CMR protocol

As described in the Introduction, the strength of CMR is its ability to capture multiple types of information about the health of the heart using a single imaging modality. However, this flexibility can be seen as a "double-edged sword": because CMR scans are sensitive to a wide range of physiologically relevant effects, each of these effects may become a confounder when attempting to capture a specific aspect of cardiac health. Consider cardiac motion—although imaging motion is essential for the assessment of cardiac function, this same process is typically treated as a troublesome generator of artifacts when collecting images for tissue characterization. The standard approach is shown in Fig. 1a, where a different dedicated pulse sequence independently targets relevant physiological processes one-by-one. Here it can be seen that cine images and maps of quantitative parameters like T_1, T_2, T_2* or ECV are each acquired using a specialized pulse sequence [6], usually during breathholds. This chain of serial acquisitions can lead to potential biases from un-mapped parameters, lack of co-registration between maps and images with different contrasts, and long scan times. These individual pulse sequences are carefully (sometimes precariously) timed to remove or ignore confounding effects—after which the technologist must go back and target these previous "confounders" by applying a different dedicated pulse sequence in a later scan. For example, T_1 recovery is treated as a confounder in cine, T_2 mapping, and perfusion scans, but is the sole focus of T_1 mapping scans because of its utility as a biomarker for fibrosis, fat infiltration, iron deposition, and more. This strategy to purposefully avoid collecting multiple forms of clinically useful information, and to not share common imaging information between scans, is naturally inefficient, leading to long serial exams.

An alternative to imaging using consecutive sequences is to use an *all-in-one* approach (Fig. 1b). Rather than serially interrogating one process at a time, several recently introduced imaging frameworks have shown it is possible to simultaneously image multiple processes—motion, relaxation, contrast agent dynamics—as they co-occur. The ultimate vision of an "all-in-one" CMR protocol is a single sequence that is sensitive to all clinically relevant tissue properties for a particular patient, and which collects data during free-breathing and without the need for ECG gating. Note that "all-in-one" need not be "one-for-all": this approach can be patient-centric, aiming to replace an individual patient's serial exam with a single, tailored sequence, rather than serving as a standardized examination. If acquired in 3D, volumetric imaging would eliminate the need for the collection of individual 2D slices, as the 3D volumes can be reformatted into 2D images in any orientation showing the anatomy of interest. However, 2D imaging may be considered "all-in-one" if 3D coverage is not required to answer the clinical question, e.g. monitoring a targeted region of interest with known location. The more important feature of an "all-in-one" exam is the simultaneous, interleaved acquisition of multiparametric data during motion. By jointly processing these data, maps of all relevant tissue properties can be generated along with cine images showing the motion of the heart and even respiratory-resolved images. This multiplexed imaging is attractive as an alternative to conventional CMR as it may be more efficient, easier to perform at the scanner, and produce natively co-registered images ready-made for multiparameter analysis.

The following sections will describe several recent approaches for "all-in-one" CMR, the strengths and weaknesses of these approaches, and additional challenges which must be tackled before they can be translated for clinical use.

Existing methods for "all-in-one" cardiac imaging and existing validation

Achieving all-in-one CMR requires advances in pulse sequence design, image reconstruction, and image analysis. Several imaging frameworks have been developed in recent years which combine advances in all of these areas to lay the groundwork for all-in-one imaging.

The first joint methods targeted efficient myocardial tissue characterization. Most of these early approaches were designed to sample a few contrast-weighted images, from which several parameters of interest could be derived (usually via exponential fits). Note that none of these examples enables full "all-in-one" scanning, but each demonstrates that several different types of information may be collected simultaneously, the first step towards the desired "all-in-one" CMR exam. One of the first methods to be described combined inversion recovery (IR) and T_2 preparation (T2prep) modules, commonly used to encode T_1 and T_2, into a single, free-breathing, interleaved acquisition [7] (Fig. 2). This strategy enabled co-registered maps with a spatial resolution of $1.3 \times 1.3 \times 8\,mm^3$ to be derived from a single (navigator-gated) free-breathing acquisition of ~3 min. Estimated T_1 and T_2 values were in agreement with literature values, with coefficients of variance (CoVs) of ~4.6% and ~2.6%, respectively. The combination of IR and T2prep for parametric encoding has been used in several studies [10,11,8,9], using both exponential fitting and dictionary matching, and have provided high-accuracy cardiac T_1 and T_2 quantification [12-15]. Joint T_1/T_2

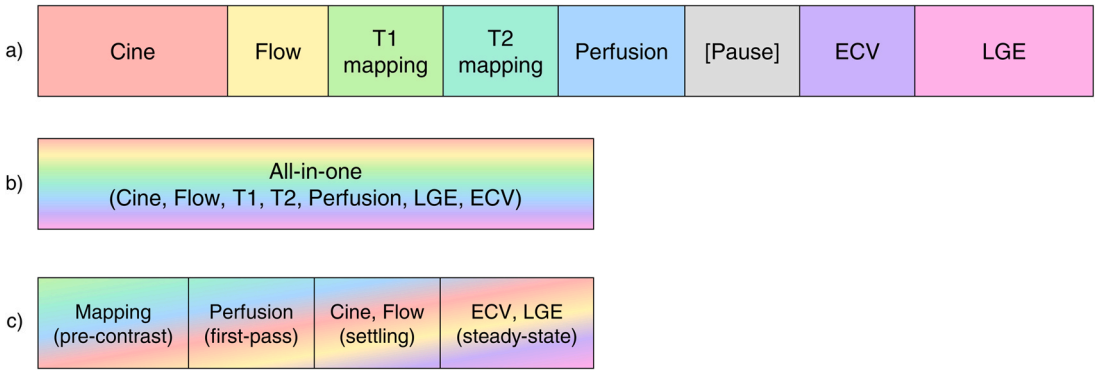

Fig. 1. Conceptual examples of the (a) one-by-one serial scan protocol and (b) all-in-one exam protocol. (c) A "tilted" all-in-one protocol further considers the limitations posed by contrast agent dynamics. ECV: extracellular volume fraction, LGE: late gadolinium enhancement.

estimation has also been developed using saturation recovery (SR) instead of IR, acquired in a single breath-hold [16], achieving a resolution of $2 \times 2 \times 8$ mm^3 with a scan time of ~13 s. Negligible biases were observed relative to saturation recovery single-shot acquisition (SASHA; ~ −9.6 ms) and T2prep-balanced steady state free precession (bSSFP; ~0.7 ms) for T_1 and T_2, respectively, along with similar precision (estimated via the standard deviation in each heart segment). A similar approach is followed in [17], further incorporating variable flip angles for increased precision, enabling the estimation of T_1 and T_2 values with a resolution of $1.4 \times 1.9 \times 8$ mm^3 in a ~11 s breath-hold. Non-significant differences were observed in T_1 relative to SASHA (~4 ms), however T_2 was significantly higher than linear-order T2prep-bSSFP (~4.6 ms); corresponding CoV were ~3.3% and ~6.7% for T_1 and T_2, respectively.

Although ECG-triggering is commonly used to freeze cardiac motion, several forms of mapping have been demonstrated in a "free-running" (albeit breath-held) approach. For example, IR and continuous bSSFP readouts have been used for T_1 and T_2 encoding, and non-rigid registration is used to account for cardiac motion [18], achieving a resolution of $1.7 \times 1.7 \times 8$ mm^3 in an ~8 s breath-hold. Only small biases were measured relative to modified Look-Locker inversion recovery (MOLLI; ~ 2 ms) and T2prep-bSSFP (~0.7 ms); CoVs were ~3.2% and 6.3% for T_1 and T_2, respectively. IR-prepared, free-running strategies have also been explored to assess both T_1 and functional information in single breath-hold [19]. By ensuring that each cardiac phase has the appropriate T_1 encoding it is possible to obtain cardiac resolved T_1 maps, at a resolution of $1.9 \times 1.9 \times 10$ mm^3 in a breath-hold of 17–23 s. T_1 values were ~7% lower than saturation pulse prepared heart rate independent inversion-recovery (SAPPHIRE) T_1 mapping, with apparent precision varying from 100–150 ms (increasing with the cardiac phase). Similar ideas have been explored to produce simultaneous T_1 mapping and cine imaging during free-breathing and without gating, using self-gated image navigators to derive respiratory and cardiac motion states and a dual flip-angle sequence to correct for B_1+ [20], a common confounding factor in parametric mapping. This approach enables the collection of maps with a resolution of $1.5 \times 1.5 \times 8$ mm^3 in a ~30 s free-breathing scan (with a positive bias of ~94 ms reported relative to MOLLI). Yet another approach for cine and cardiac resolved T_1 mapping combines the free-running IR prepared sequence with a model-based reconstruction acquired in a 16 s breathhold [21] with a resolution of $1.3 \times 1.3 \times 8$ mm^3. A positive bias of ~80 ms relative to MOLLI was observed, with an apparent precision in the range of 57–65 ms, depending on the cardiac phase. Model-based formulations allow for high acceleration factors and have demonstrated high resolution ($1 \times 1 \times 8$ mm^3) T_1 mapping in ~4 s scan time [22], with negligible biases relative to MOLLI (~20 ms) and a CoV of approximately 3%. Joint $T_1/T_2/T_2$* mapping has been demonstrated in free-breathing using SR, T2prep, multi-gradient-echo and navigator gating, for 2x2x8 mm^3 resolution multi-parametric mapping in a ~26.5 s scan [23]. Minor differences were observed relative to SASHA (~30 ms), T2prep-bSSFP (~0 ms) and multi-echo-gradient-echo (~1.5 ms), for T_1, T_2 and T_2*, respectively; corresponding precisions were ~68 ms, ~1.1 ms and ~ 3.3 ms.

The methods mentioned above can be used to collect multiple forms of tissue property information from 2D slices. However, expanding on these 2D approaches, there have been developments for 3D multi-parameter mapping. Full heart coverage is generally desirable in CMR, but further sequence considerations must be addressed, as the length of the breath-holds that would be required for clinically-acceptable resolutions and coverage are not feasible. Sequences that employ cardiac triggering and/or respiratory gating can be used, but may suffer from inaccuracies in the presence of arrhythmias and/or impractical scan times. Nevertheless, full left ventricular T_1/T_2 mapping (with between 10–13 slices to achieve full coverage) has been obtained in a single breathhold using IR/T2preps [24,25]; Fig. 3 shows an example of 3D maps collected using the 3D-quantification using an interleaved Look-Locker acquisition sequence with a T2-preparation pulse (3D-QALAS) approach. Preliminary clinical evaluation demonstrated 3D T_1 and T_2 mapping with a resolution of $2 \times 2 \times 12$ mm^3 in a ~17 s breath-hold, with negligible biases for T_1 (~ −7.3 ms) and T2 (~0.1 ms) [26]. SR/T2prep sequences have also been evaluated for 3D free-breathing T_1/T_2, in combination with navigator gating and fat suppression [27,28]. In such an approach, 3D T_1 and T_2 maps can be obtained with a resolution of $1.5 \times 1.5 \times 16$ mm^3 in a ~8 min scan time. Both T_1 and T_2 values were in agreement with literature values, with reported CoVs of ~6.0% and 10.2% for T_1 and T_2, respectively. Isotropic water/fat separated T_1 and T_2 maps have also been obtained in 3D under free-breathing using IR/T2preps and image navigators for respiratory motion correction [29], achieving a $2 \times 2 \times 2$ mm^3 resolution in a ~9 min scan time. A positive bias relative MOLLI was reported (~101 ms), along with a minor bias relative to T2prep-bSSFP (~ −0.8 ms); corresponding precisions were 55 ms and 3.9 ms for T_1 and T_2, respectively; example T_1 and T_2 maps along with fat and water images generated using this technique are shown in Fig. 4. Isotropic T_1 and T_2 mapping and cine have also been demonstrated in free-breathing using a 3D self-navigated golden radial trajectory and respiratory motion correction, offering a $2 \times 2 \times 2$ mm^3 resolution in an ~11 min scan time [30]. This study also reports a positive bias relative to MOLLI (~140 ms) and a negative bias relative to T2-gradient- and spin-echo (GraSE; (~ −4.4 ms), with precisions of ~30 ms and ~1.9 ms for T_1 and T_2, respectively.

Unlike the approaches described above, techniques like magnetic resonance fingerprinting (MRF) follow a different paradigm, where unique information about tissue properties is collected throughout the pulse sequence [31]. MRF leverages incoherent artifacts due to irregular spatial encoding along with dictionary template matching to enable parametric mapping from highly undersampled data [32-34]. Cardiac MRF [35] was initially proposed for mapping T_1 and T_2 in 2D

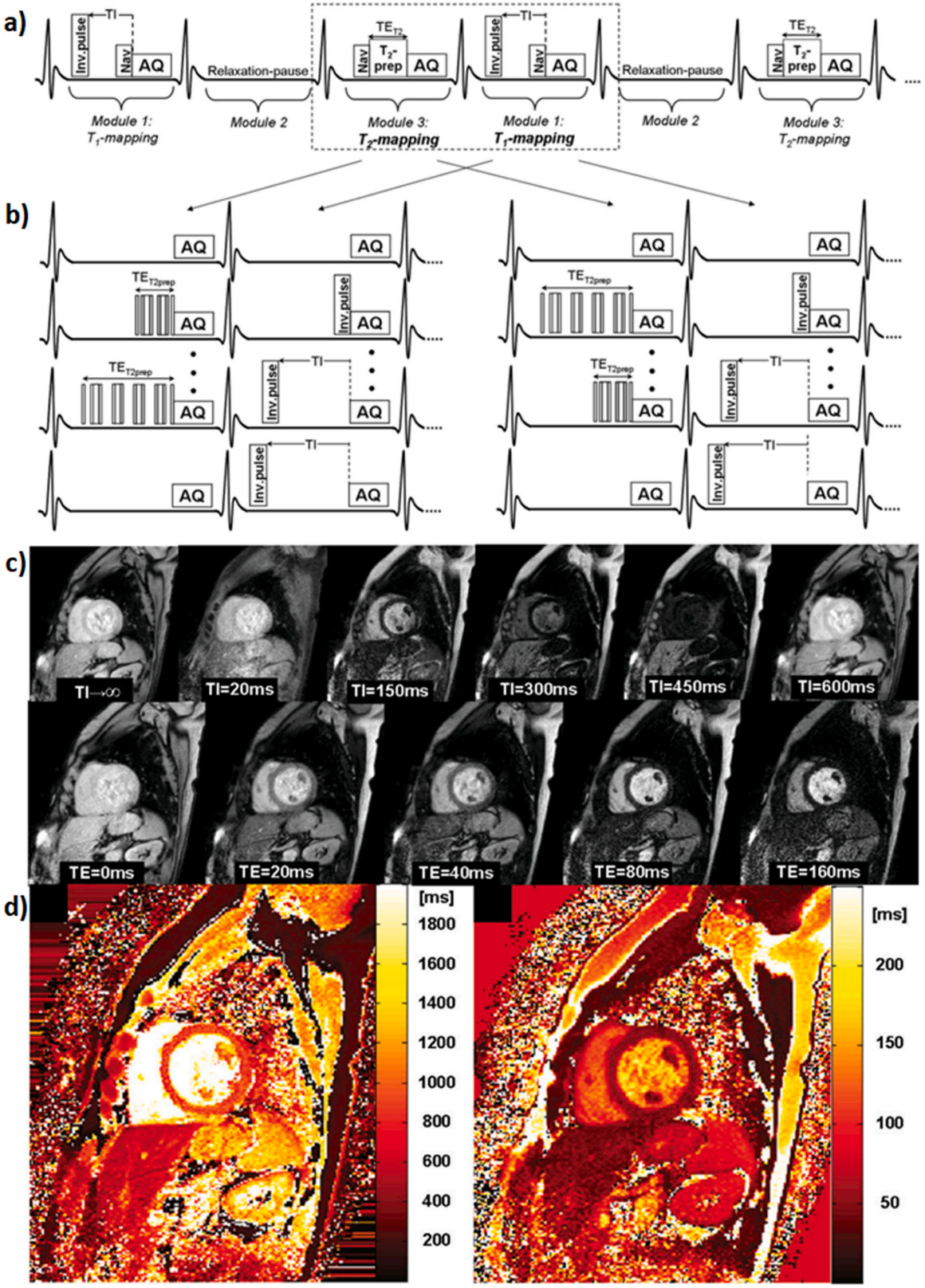

Fig. 2. Interleaved T_1/T_2 cardiac parametric mapping. a and b) The joint T_1/T_2 mapping framework employs a combination of inversion recovery and T_2 preparation pulses to encode T_1 and T_2, and respiratory navigators to compensate for breathing motion. c) T_1 and T_2 contrast weighted images acquired at different heartbeats that are used to map T_1 and T_2 d) Representative T_1 and T_2 maps obtained. AQ: acquisition; Nav: respiratory navigator; TE: echo time; TI: inversion time Figure reproduced with permission from [7].

using an IR/T2prep sequence similar to [7], but with a model-based reconstruction using dictionaries simulated using the Bloch equations (Fig. 5). The original MRF approach in the heart was used to estimate T_1 and T_2 at a resolution of $1.6 \times 1.6 \times 8\,mm^3$ in a ~16 s breath-hold. Minimal differences were reported relative to MOLLI (~1 ms) and T2prep-bSSFP (~−2.6 ms); corresponding precisions were ~71 ms

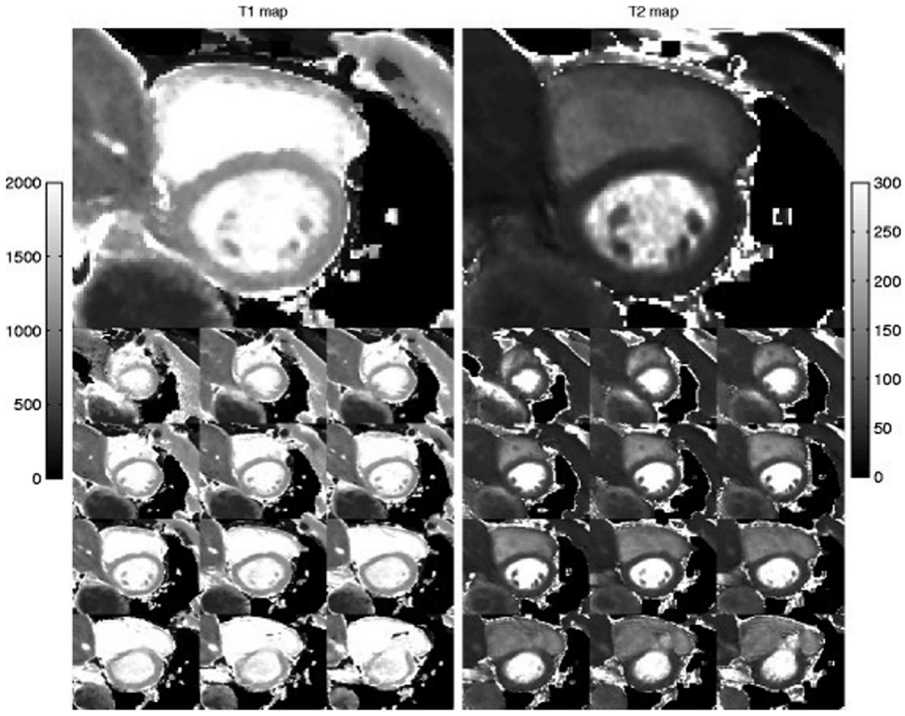

Fig. 3. 3D-QALAS images from a healthy volunteer. The thirteen 3D-QALAS short axis slices T_1 maps (left) and T_2 maps (right) of the left ventricular myocardium are shown. Slice 8 is shown on a larger scale. The gray scale indicates 0–2000 ms for T_1 and 0–300 ms for T_2.. 3D-QALAS: 3D quantification using an interleaved Look-Locker acquisition sequence with a T2-preparation pulse.
Figure reproduced with permission from [25].

and ~5.5 ms for T_1 and T_2, respectively. The impact of slice profile and B1+ errors in cardiac MRF has been studied, revealing that negligible biases are produced when the sequence employs small flip angles [36]. The flexibility of the MRF framework has facilitated the development of several different forms of multi-parametric mapping in the heart [37-39]. 2D Water/fat separated T_1/T_2 maps collected in a breath-hold have been demonstrated using both radial [40] and rosette [41] trajectories, showing good agreement with conventional (separate) mapping

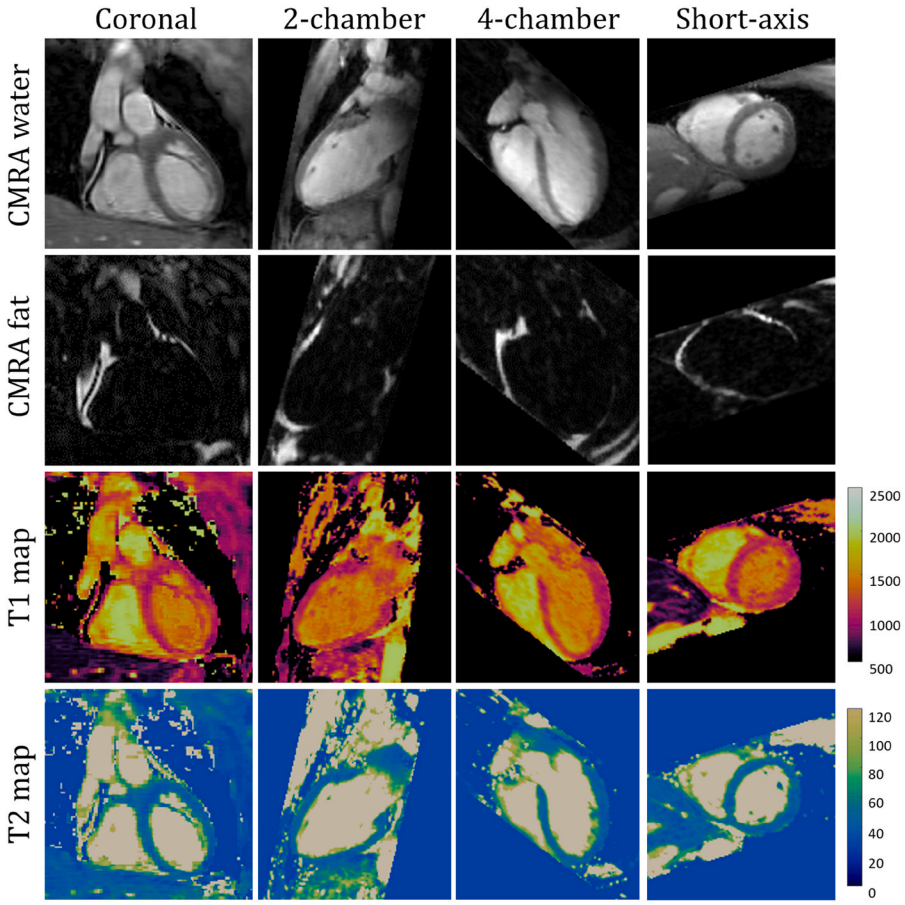

Fig. 4. Co-registered 3D bright-blood dataset (T_2-prepared), fat volume, and T_1 and T_2 maps obtained with the proposed approach and reformatted in different orientations (coronal, 2-chamber, 4-chamber, and short-axis) for 1 representative healthy subject. Good depiction of cardiac structure such as right coronary artery and papillary muscles is achieved in the bright-blood dataset. Good water/fat separation is obtained across the whole 3D volume, and uniform T_1 and T_2 quantification are shown in the different orientations. CMRA: contrast magnetic resonance angiography
Figure reproduced with permission from [29].

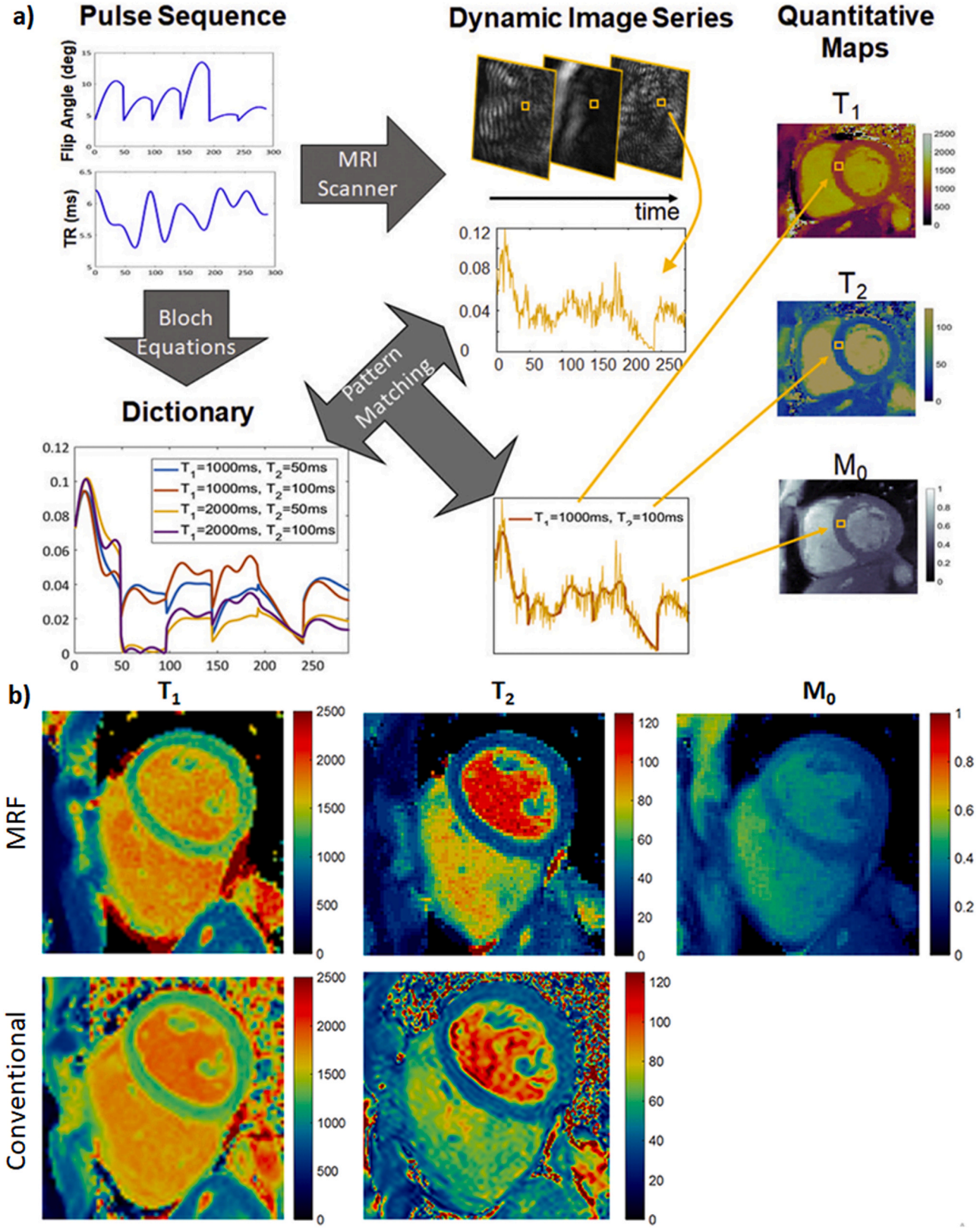

Fig. 5. Cardiac MR Fingerprinting for multi-parametric mapping. a) The MRF framework employs Bloch equations to predict the expect signal evolution of a set of tissues (dictionary) for a given sequence. Highly undersampled dynamic images are matched to this dictionary to immediately retrieve the underlying parameters (e.g. T_1/T_2). b) Representative parametric maps obtained with MRF compared with conventional MOLLI and T_2-prepared maps.
Figure reproduced with permission from [37]. MRF: magnetic resonance fingerprinting; MOLLI: modified Look-Locker inversion recovery.

methods. The former approach [40], acquired maps with a resolution of $2 \times 2 \times 8$ mm^3 in a ~15 s breath-hold. T_1 biases of ~ − 80 ms and ~20 ms were observed relative to SASHA and MOLLI, and a bias of ~ − 9 ms was observed relative to T2-GraSE; corresponding precisions were ~49 ms and ~4.6 ms for T_1 and T_2, respectively. In the latter approach [41], a resolution of $1.6 \times 1.6 \times 8$ mm^3 was achieved in ~15 s breath-hold. Similar results were observed, with a positive bias reported relative to MOLLI (~130 ms), and a negative bias relative to T2prep-fast low angle shot (FLASH) (~ −6 ms). Improved coverage for T_1/T_2 MRF has been obtained with simultaneous multi-slice acquisitions [42], where three slices can be mapped together in a single breath-hold while maintaining similar performance to previous methods. In preliminary studies on healthy subjects [43], T_1/T_2 cardiac MRF has compared favorably against reference methods in terms of image quality assessment. Initial studies in non-ischemic cardiomyopathy patients have shown similar mapping performance between MRF and corresponding references (despite the shorter scan time of MRF) [44]. T_1/T_2/PDFF (proton density fat fraction) cardiac MRF has also been validated in healthy subjects and patients, indicating improved mapping for MRF relative to references due to the removal of fat as a confounding factor from the water-only T_1 and T_2 maps [45]: [46]. This framework has been further extended to $T_1/T_2/T_2$*/PDFF mapping in a single breath-hold using an increased echo-train for T_2* encoding, enabled by a cardiac motion corrected acquisition window [47]. Here, maps with a resolution of 2x2x8 mm^3 were acquired in an ~18 s breath-hold. Biases were measured versus MOLLI (~90 ms), T2-GraSE (~ −8 ms), 8-echo GRE (~ −4.4 ms) and 6-echo GRE (~0.5%) for T_1, T_2, T_2 * and PDFF, respectively. Corresponding precisions were, ~47 ms, ~4.1 ms, ~7.8 ms and ~2.7%. $T_1/T_2/T_{1\rho}$ cardiac MRF with a resolution of 2x2x8 mm^3 has also been demonstrated using a combination of IR/T2prep/spin lock preparations in a ~16 s breath-hold [48]. A bias of ~52 ms was reported relative to MOLLI, ~ − 10 ms relative to T2-GraSE and ~ − 7.4 ms relative to $T_{1\rho}$-TFE, for T_1, T_2 and $T_{1\rho}$, respectively; corresponding CoV were ~6.0%, ~9.3% and ~12.6%. The MRF framework has also been used to develop simultaneous T_1 and T_2 mapping along with cine imaging using spiral [49] and radial [50] trajectories within a breath-hold, where both have reported good agreement with reference methods. In the former, encoding is achieved via IR and T2preps, followed by registration prior to dictionary matching. In the latter, encoding is achieved with IR and high flip angles, using only cardiac resolved reconstructions. T_1 and T_2 mapping with MRF has also been extended to 3D free-breathing acquisitions [51,52], where elastic motion fields are estimated from the data itself and used to correct for the respiratory motion. Here, 3D T_1 and T_2 maps with a resolution of $2 \times 2 \times 8$ mm^3 are obtained in ~7 min scan time. A positive bias of ~25 ms and ~ − 8 ms was observed relative to MOLLI and T2-GraSE; corresponding precisions were ~61 ms and ~4.7 ms for T_1 and T_2, respectively.

Virtually all cardiac MR applications need to address respiratory and cardiac motion. In the context of parametric mapping, these are generally managed with a combination of ECG-triggering and breath-holds, although some approaches employ gating or motion correction. However, the desired “all-in-one” approach would not be complete without the ability to assess at least cardiac motion in place of standard cine imaging. In an “all-in-one” protocol, this challenge can be tackled by noting that all the varying contrasts and motion states belong to the same underlying heart, and therefore are connected. Multitasking [57] exploits this redundancy by formulating the reconstruction of each of these factors as a tensor, where each dimension captures a main mode of variation in the data (e.g. spatial information, T_1 contrast, T_2 contrast, respiratory motion, cardiac motion, etc.) (Fig. 6). As such, each image in this tensor (i.e., with a given contrast, in a given motion state) can be written as a linear combination of the images from all other contrast/motion states, as long as the tensor’s subspaces are known (which can generally be estimated either by theoretical models or from the data itself). This Multitasking formulation has enabled respiratory and cardiac resolved T_1/T_2 mapping under free-breathing and without ECG, turning the challenge of motion into a data feature. The first multitasking study provided (cardiac-resolved) T_1/T_2 maps at a resolution of $1.7 \times 1.7 \times 8$ mm^3 in an ~88 s free-breathing scan. A bias of ~ − 31 ms was reported relative to MOLLI and ~2.5 ms relative to T2prep-bSSFP; corresponding CoVs were ~6.3% and ~11.4% for T_1 and T_2, respectively. Joint T_1/B_1 corrected multitasking has been developed using a dual flip angle approach, for improved T_1 mapping with a $1.7 \times 1.7 \times 8$ mm^3 resolution in ~60 s; reported T_1 values ~350 ms higher than MOLLI (more in line with typical SASHA values), with a CoV of ~4.4% [58]. This approach has been combined with simultaneous multi-slice T_1/T_2, allowing for respiratory and cardiac motion resolved T_1/T_2 in three slices from a 3 min scan [59]. Here, T_1 and T_2 values were slightly lower than MOLLI (~ −25 ms) and T2prep-FLASH (~ −1.2 ms), with corresponding CoVs of ~4.7% and 8.9% for T_1 and T_2, respectively. Motion-resolved T_1 and ECV with Multitasking have been validated with infarction patients in a preliminary study, demonstrating good agreement with the reference [60], as well as histologically in a rat model of heart failure with preserved ejection fraction, correlating with Masson’s trichrome stain for fibrosis [61]. Motion-resolved whole left ventricular diffusion tensor imaging has been achieved with Multitasking, using slice selective excitations, multi-slice EPI readouts, and auxiliary respiratory motion correction [62]. Dynamic T_1 mapping for cardiac-resolved quantitative perfusion imaging with Multitasking showed high repeatability in healthy subjects [57]. Finally, cardiac resolved $T_1/T_2/T_2$*/PDFF has also been demonstrated with Multitasking [63], using IR and hybrid T2IR modules, radial readouts, and multi-echo GRE with a resolution of $1.7 \times 1.7 \times 8$ mm^3 in a scan time of ~150 s. This study reported a bias of ~60 ms relative to MOLLI, ~ − 3.1 ms relative to T2prep-GRE, ~1.3 ms relative to 8-echo GRE and ~ − 1.1% relative to 6-echo GRE for T_1, T_2, T_2* and PDDF, respectively. Corresponding CoVs were ~5.1%, ~6.7%, ~14.4% and ~72.3%. While quantitative cardiac multitasking has only been reported for 2D and multi-slice 2D imaging, qualitative 3D imaging [64] and quantitative proofs-of-concept [65] have been demonstrated in the heart, and quantitative 3D versions have been validated in other moving organs [66]. Given that more conventional quantitative mapping approaches have been used to collect 3D maps of multiple tissue properties, including T_1 [67], T_2 [68], and $T_{1\rho}$ [69], the transition from 2D to 3D all-in-one acquisitions is fairly straightforward.

The complexity of the acquisition and reconstruction of “all-in-one” processes, along with the need for patient-specific dictionaries have challenged their clinical deployment. However, recent developments in artificial intelligence/deep learning (AI/DL) have been incorporated to overcome some of these challenges [53]. As an example, deep learning has been used to reduce the time needed to generate cardiac MRF dictionaries from 158 s to 0.8 s [54]. Deep learning has been used to bypass the need for dictionaries in MRF altogether, resulting in shorter reconstruction times; in the case of spiral MRF, the reconstruction time was only 76 ms with DL compared to 380 s with conventional approaches [55]. While not yet feasible for clinical use due to the computational time needed, deep image prior reconstructions of cardiac MRF data may enable data collected over shorter breathhold durations (5 heartbeats instead of 15) and diastolic scan windows (150 ms instead of 250 ms) to be processed into more accurate tissue property maps than those generated using non-AI approaches [56]. Future combinations of AI/DL techniques may eventually enable more tissue properties to be extracted from more rapidly collected datasets in a subsecond reconstruction time, further assisting in clinical translation.

Advantages and disadvantages of all-in-one cardiac exams compared with conventional CMR

All-in-one CMR exams have the potential to offer an array of benefits for patients, radiographers, and physicians due to shorter scan

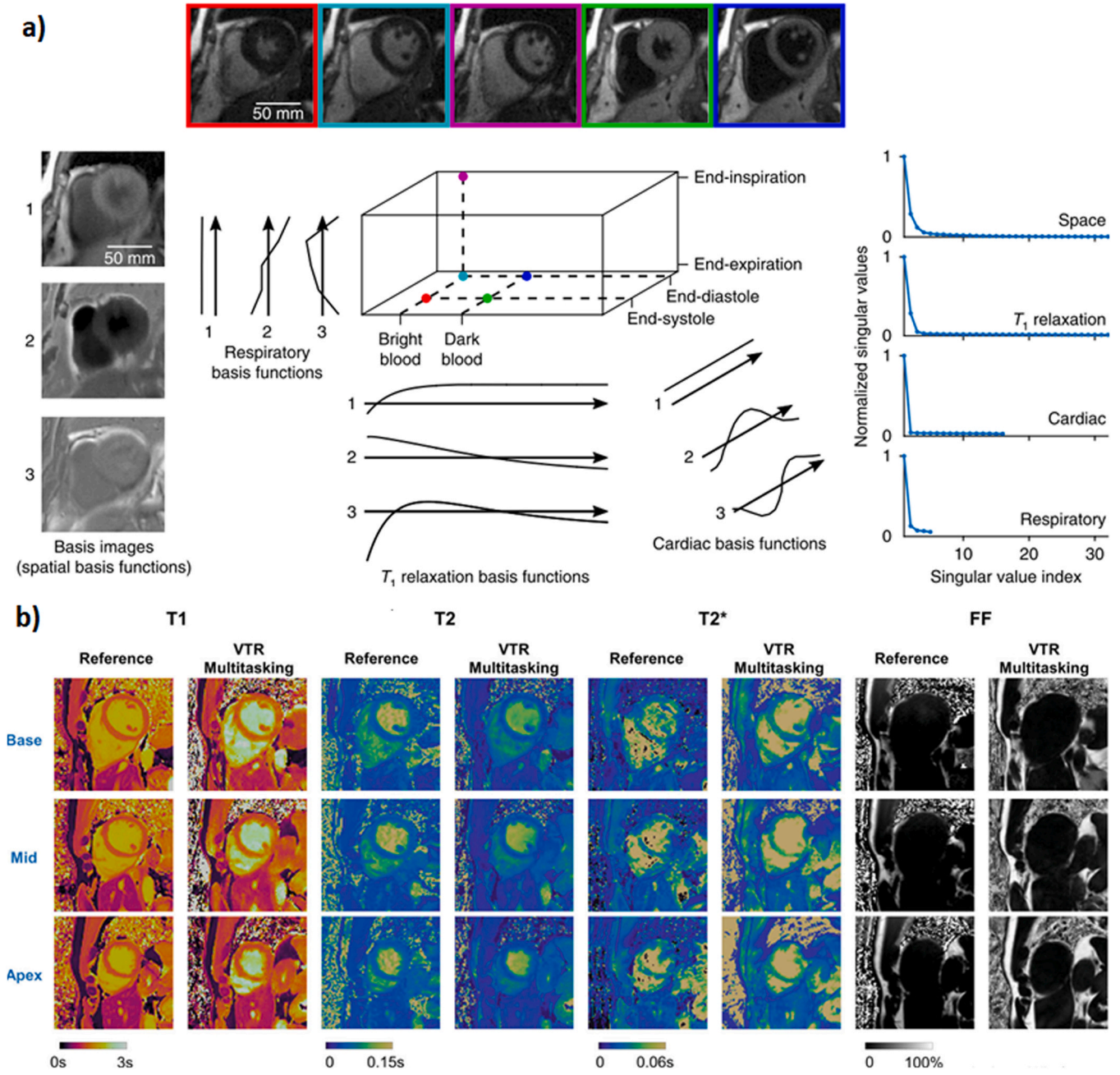

Fig. 6. Multitasking for motion resolved multi-parametric mapping. a) Data from varying contrast and motion states are jointly reconstructed within a tensor formulation, establishing each motion/contrast state as a linear combination of all others, enabling mapping in free-breathing without cardiac triggering. b) Representative cases of multitasking for $T_1/T_2/T_2^*$ /PDFF compared to corresponding (separate scan) conventional approaches.

times, simpler patient preparation and localization, and less complex multiparametric analysis, respectively. However, some aspects of an all-in-one examination may be more challenging than when working with a conventional CMR protocol. Thus, advantages and disadvantages of this approach must be carefully considered when moving to clinical application. An overview of advantages and disadvantages of "all-in-one" type acquisitions is given in Table 1, and the most important are discussed below.

Advantages of all-in-one exams

All-in-one exams are specifically designed to acquire a range of contrasts from a single scan; because all reconstructed images are based on the same data, they are intrinsically co-registered. Depending on the implementation, this can mean obtaining co-registered viability and tissue characterization scans, or motion-resolved acquisitions for functional and viability imaging, or a whole range of other properties. Obtaining all data in a co-registered manner allows for straightforward cross-evaluation of different contrasts, which may substantially ease the evaluation and post-processing of the images. In particular, with the emergence of ever more powerful machine learning-based post-processing techniques [70], the co-registered and unified data basis of all-in-one exams may be key to facilitating reliable and automatic diagnosis in the future [71,72].

In all-in-one sequences, many relevant dimensions of physiological and signal variation can be extracted from a single dataset. This feature can be used to circumvent the need to control for these factors. For example, respiratory motion-resolved acquisitions alleviate the need for breath-holds and the accompanying scan time restrictions, whereas cardiac phase-resolved acquisitions can circumvent the need for ECG

Table 1
Advantages and Disadvantages of an "All-in-One" CMR protocol.

Advantages	Disadvantages
Co-registered Tissue Property Maps All-in-one methods enable co-registered and unified quantification of multiple tissue property maps from a single scan	**Quantification Dependency** All-in-one methods require careful consideration of how the sequence design affects the contrast and quantification accuracy/precision, as different readouts, preparation modules, trajectories and imaging volumes may introduce confounding factors or dependencies
Flexible Sequence Design All-in-one methods enable more flexible and customized sequence designs with minimized scan times by avoiding the need for rest-periods and using all collected information for joint reconstruction of multiple maps	**Only resilient against the modelled factors** All-in-one methods suffer from compromised accuracy if relevant effects contributing to the acquired signal are not explicitly modelled or corrected
Acquisition efficiency/Synergy All-in-one methods allow for optimal use of redundancies and cross-utilization of contrast information for high scan time efficiency	**Computational complexity and artifact sensitivity** All-in-one methods process a large, single set of data, which may pose computational challenges and render the acquisition sensitive to corruption by artifacts or motion

triggering and measurements of the longitudinal relaxation time can often replace recovery periods. Resolving the dimensions of variability may enable more flexible sequence designs in terms of scan times or contrast weightings beyond conventional signal models. This potentially allows for tailoring the sequence weightings and tuning the desired precision or image quality in different contrasts to the specific use case. In short, the acquisition could be designed to last only as long as necessary to collect the required information for the clinical question, resulting in minimized scan times for each specific patient.

In all-in-one acquisitions, all data is processed together for image reconstruction. Thus, the ideal use of redundancies among the contrasts can be exploited. For example any image acquired in diastole can be used to assist in the characterization of diastolic function. However, in conventional protocols, the only images used for functional analysis are the cines; other high resolution diastolic images are ignored. Another example in traditional MR methods is that similar contrast information is reacquired over and over again, for example the fully relaxed magnetization M_0, which is often important for quantification. All-in-one exams provide a unique opportunity here to cross-utilize this information for more than just one contrast, enabling to extract comprehensive multi-parameter information at the upper limit of achievable SNR per scan time.

Disadvantages of all-in-one exams

In all-in-one acquisitions, all aspects of the sequence are tightly coupled to the contrasts that can be extracted. Thus, the acquisition itself may affect quantitative measurements by necessitating to resolve more dimensions or by introducing confounders. For example, with conventional quantitative techniques in the heart, the contrast is often created through the use of preparation modules such as inversion or T2prep modules, the imaging readout is decoupled from the contrast preparation to obtain optimal image quality. In all-in-one acquisitions, the imaging readout and its effect on the magnetization are intertwined. For example, the use of bSSFP readouts is only possible when accounting for T_2 and off-resonance effects, while many spoiled acquisition readouts can only be used accurately when accounting for B1 + inhomogeneities. In another example, the use of preparation pulses, such as inversion pulses, may introduce $T_{1\rho}$ decay during the pulse or other imperfections as confounders. Complex trajectories may lead to differential contrast depending on the amount of spoiling or rewinding. Similarly, the imaging volume (2D vs 3D) directly affects what contrasts can be obtained with the all-in-one technique. For example, 3D imaging might be required in order to accurately model the magnetization history of tissues affected by cardiac or respiratory motion, or flow.

The fact that all-in-one exams sample a great amount of data to capture a variety of physiological parameters can cause a computational bottleneck. All of the data must be processed together, which for some models comes at the price of high computational complexity. This often necessitates either simplifications or leads to extraneously long reconstruction times. What is more, as the entire scan forms a single data set, it is prone to corruption. Problems with various artifacts, such as radiofrequency (RF) zippers, can contaminate the entire scan, and if these errors go unnoticed, may require that the entire scan be repeated. This may be particularly important in the case of motion artifacts, where the effect size can be exacerbated over longer time spans, due to position drifts or patient motion. Thus, the acquisition of a continuous data block may prove both to be a time advantage but also a risk and a bottleneck in realizing quick and reliable cardiac CMR in the future.

Open needs before an "all-in-one" protocol could be deployed

Despite the significant advances in pulse sequence design and information extraction methods described above, there are still challenges to overcome before all-in-one protocols could be used to replace serial protocols in the clinic. These open problems are opportunities for both technical and clinical research as well as commercial development.

Full all-in-one development

In a true all-in-one exam, a single scan would replace every measurement currently used as part of today's clinical protocols. By this standard, even the most highly-multiplexed sequences available today only achieve "several-in-one" scanning. For example, it is now possible to combine cine imaging with native multiparameter relaxation mapping, but these methods have not been integrated with high-dimensional flow and contrast-enhanced imaging. Current techniques will need to be augmented to either address contrast agent dynamics or to integrate non-contrast replacements such as arterial spin labeling or virtual enhancement from native multiparameter images [73]. Although cardiac motion can be captured in emerging high-dimensional mapping techniques, these sequences will not replace current clinically available cine protocols until they are available as whole-heart protocols with spatiotemporal resolution matching that of standard cine sequences.

An important consideration in such an "all-in-one" protocol is the administration of contrast agents. Non-contrast protocols have no fundamental limitation to how many scans can be multiplexed into one. However, contrast scans such as perfusion and LGE imaging are a core part of clinical CMR offerings. These types of scans have the potential to be accommodated in all-in-one protocols by treating the wash-in and wash-out of contrast agent throughout the entire exam as a single non-repeating dynamic process which overlaps with the faster repeating dynamic processes of motion, relaxation, and flow. One such construction (Fig. 1c) groups native tissue characterization into a pre-contrast phase, perfusion into the first-pass of contrast agent, cine and

flow during settling of contrast agent, and ECV mapping and LGE into the steady-state contrast phase. While this is one option that has been proposed, the optimal timing of contrast agent delivery and reconstruction approach for extracting relevant information has yet to be fully explored.

Clinical validation and integration

Prior to wide clinical deployment, methods must be extensively validated in heterogenous multicenter studies, and be seamlessly integrated into existing clinical imaging workflows. Achieving this integration will require advances in fast in-line image reconstruction, efficient picture archiving and communication system (PACS)-compatible storage, and high-dimensional display tools. Image reconstruction speed has already dramatically improved in a few short years, especially with the use of supervised deep learning architectures [54,74,75,9]. However, supervised deep learning methods heavily rely on access to large volumes of high-quality training data, which may not be readily available. Further, these methods may not generalize well to different imaging contexts or diverse patient populations outside of the distribution of their training data. Recognizing these limitations, some researchers have explored unsupervised or self-supervised methods [53,56,76,77]. Although these methods are typically slower than their supervised counterparts, their independence from training data may offer greater flexibility across different contexts. Regardless of the supervision strategy, the field would benefit from a shift toward explainable AI that can provide more interpretable results, confidence estimations, and understandable algorithms, increasing trust for wider clinical adoption. In-line integration of deep learning reconstruction methods into scanner image reconstruction pipelines is currently underway through flexible reconstruction platforms such as Gadgetron and similar vendor-provided options [78]. However, the generalizability and portability of these in-line workflows to multiple centers is still not fully established.

As all-in-one protocols increase in dimensionality to incorporate additional contrasts, flow, and contrast agent dynamics, the number of images they generate per scan can grow exponentially. It will no longer be practical to store DICOMs of every individual image. However, all-in-one imaging methods already leverage low-dimensional models (e.g., nonlinear physical models, sparse representations, and low-rank decompositions) during image reconstruction to generate images from limited k-space data. These same low-dimensional models could be used as compressed storage formats. This would constitute lossless compression of the reconstructed images whenever the storage model matches the model already imposed during image reconstruction. In practice, digital imaging and communications in medicine (DICOM) containers could store model parameters—parameter maps for physics models, nonzero values and locations in the transform domain for sparse models, and decomposed factors for low-rank models—and quickly decompress images on-the-fly as specific image contrasts or motion states are requested by the viewer.

With these increases in dimensionality, further challenges also arise in image display [79]. New interfaces to handle multiple parameters and time dimensions should be integrated into display software. Image fusion of synchronized, co-registered images should be established to allow simultaneous multiparameter reading. Multichannel colorspaces such as red, green and blue (RGB) and cyan, magenta, yellow and key (CMYK) offer relatively straightforward parameter fusion by assigning one parameter per channel, but can only represent three and four parameters, respectively, which is soon to be out-paced by all-in-one protocols. In the longer term, establishing a conversion from multiple complementary biomarker maps into physiological maps (e.g., fibrosis, edema maps) would simplify image display while also offering easier interpretation for clinical decision-making.

Leveraging the full information of all-in-one protocols

To fully unlock the potential of all-in-one imaging, approaches to extract useful clinical information in the interactions between parameters could also be explored. For example, while a cine T_1 mapping sequence could simply be analyzed along a cardiac dimension to measure function and along a T_1 recovery dimension to measure T_1, there is potentially valuable information in their interactions: changes in apparent T_1 over the course of the cardiac cycle may reflect changes in myocardial blood flow and volume that are not measurable by serial cine imaging and T_1 mapping alone. The addition of a cardiac phase dimension or other "arrhythmia dimensions" may bring opportunities to explore interactions between parameters and ectopic variations or loading intervals [80,81]. Respiratory dimensions could go beyond the comfort of free-breathing to also allow analysis of cardiorespiratory interactions [82]. As the amount of information to be extracted from the data increases, so does the complexity of the computational problems. Thus methods including artificial intelligence/machine learning will become increasingly important [54]. AI/ML approaches for designing appropriate data collection strategies [83] and assessing large numbers (> 4) of tissue properties from multi-dimensional data [74,84,85] have already been demonstrated. Specialized analysis, e.g., through artificial intelligence, may be capable of extracting such nuanced information for enhanced diagnosis, risk prediction, and therapy monitoring. Fortunately, all-in-one images appear ready-made for AI: images are already co-registered, synchronized, and resolution-matched, and can be input into algorithms either directly as images or in the low-dimensional feature spaces already used for image reconstruction and storage. While powerful, these AI/ML approaches are still an area of active exploration, as the demands on the reconstruction continually grow to enable more types of information (tissue property measurements and motion estimation) to be collected in shorter scan times (ideally < 1 min in a free-breathing, ungated 3D scan), with higher degrees of accuracy. Once established, they will require rigorous testing in a variety of clinical settings [86], which may be slowed by the current lack of rapid prototyping pipelines.

Conclusion of part 1

"All-in-one" CMR is a novel approach for efficient cardiovascular magnetic resonance, but there are many steps which must be taken before these methods can be adopted in place of standard CMR examinations. Another alternative approach which may be used to accelerate CMR scans is "real-time" imaging; these methods will be the subject of Part 2 of this manuscript.

Declarations

- Ethics approval and consent to participate: Not applicable
- Consent for publication: Not applicable
- Availability of data and materials: Not applicable
- Competing interests: Not applicable
- Funding: SW and AA acknowledge funding by the NWO (STU.019.024) and the Delft Health Initiative (Health Technology Programme). Authors' contributions: AC, GC, AA, SW, JA, DP, and NS were substantially involved in the conception, research, and writing of the manuscript. All authors read and approved the final manuscript.

CRediT authorship contribution statement

Peters Dana: Conceptualization, Writing – original draft, Writing – review & editing. **Artico Jessica:** Conceptualization, Writing – original draft, Writing – review & editing. **Weingärtner Sebastian:** Conceptualization, Writing – original draft, Writing – review & editing. **Arami Ayda:** Conceptualization, Writing – original draft, Writing –

review & editing. **Cruz Gastao:** Conceptualization, Writing – original draft, Writing – review & editing. **Seiberlich Nicole:** Conceptualization, Writing – original draft, Writing – review & editing. **Christodoulou Anthony G.:** Conceptualization, Writing – original draft, Writing – review & editing.

Declaration of Competing Interest

The authors declare the following financial interests/personal relationships which may be considered as potential competing interests: Sebastian Weingaertner reports financial support was provided by NWO (STU.019.024) and the Delft Health Initiative (Health Technology Programme). Ayda Arami reports financial support was provided by NWO (STU.019.024) and the Delft Health Initiative (Health Technology Programme). If there are other authors, they declare that they have no known competing financial interests or personal relationships that could have appeared to influence the work reported in this paper.

Acknowledgements

Not applicable.

References

[1] Pennell DJ, Sechtem UP, Higgins CB, Manning WJ, Pohost GM, Rademakers FE, van Rossum AC, Shaw LJ, Yucel EK. SSociety for cardiovascular magnetic resonance/european society of cardiovascular imaging/american society of echocardiography/society for pediatric radiology/north american society for cardiovascular imaging guidelines for the use of cardiovascular magnetic resonance in pediatric congenital and acquired heart disease : endorsed by the american heart association. J Cardiovasc Magn Reson 2004;25(21):1940–65. https://doi.org/10.1016/j.ehj.2004.06.040. PMID: 15522474.

[2] Kramer CM, Barkhausen J, Bucciarelli-Ducci C, et al. Standardized cardiovascular magnetic resonance imaging (CMR) protocols: 2020 update. J Cardiovasc Magn Reson 2020;22:17. https://doi.org/10.1186/s12968-020-00607-1.

[3] Captur G, Manisty C, Moon JC. Cardiac MRI evaluation of myocardial disease. Heart 2016;102(18):1429–35. https://doi.org/10.1136/heartjnl-2015-309077. Epub 2016 Jun 27. PMID: 27354273.

[4] Raman SV, Markl M, Patel AR, Bryant J, Allen BD, Plein S, Seiberlich N. 30-minute CMR for common clinical indications: a Society for Cardiovascular Magnetic Resonance white paper. J Cardiovasc Magn Reson 2022;24(1):13. https://doi.org/10.1186/s12968-022-00844-6. PMID: 35232470; PMCID: PMC8886348.

[5] Friedrich MG. Steps and Leaps on the Path toward Simpler and Faster Cardiac MRI Scanning. Radiology 2021;298(3):587–8.

[6] Messroghli DR, Moon JC, Ferreira VM, et al. Clinical recommendations for cardiovascular magnetic resonance mapping of T1, T2, T2 and extracellular volume: a consensus statement by the Society for Cardiovascular Magnetic Resonance (SCMR) endorsed by the European Association for Cardiovascular Imagin. J Cardiovasc Magn Reson 2017;19(1):24. https://doi.org/10.1186/s12968-017-0389-8.

[7] Blume U, Lockie T, Stehning C, et al. Interleaved T1 and T2 relaxation time mapping for cardiac applications. J Magn Reson Imag 2009;29:480–7. https://doi.org/10.1002/jmri.21652.

[8] Shao J, Zhou Z, Nguyen KL, Finn JP, Hu P. Accurate, precise, simultaneous myocardial T1 and T2 mapping using a radial sequence with inversion recovery and T2 preparation. NMR Biomed 2019;32:1–12. https://doi.org/10.1002/nbm.4165.

[9] Shao J, Ghodrati V, Nguyen KL, Hu P. Fast and accurate calculation of myocardial T1 and T2 values using deep learning Bloch equation simulations (DeepBLESS). Magn Reson Med 2020;84:2831–45. https://doi.org/10.1002/mrm.28321.

[10] Henningsson M. Cartesian dictionary-based native T1 and T2 mapping of the myocardium. Magn Reson Med 2022;87:2347–62. https://doi.org/10.1002/mrm.29143.

[11] Jarkman C, Carlhall CJ, Henningsson M. Clinical evaluation of the Multimapping technique for simultaneous myocardial T1 and T2 mapping. Front Cardiovasc Med 2022:960403.

[12] Messroghli DR, Radjenovic A, Kozerke S, Higgins DM, Sivananthan MU, Ridgway JP. Modified Look-Locker inversion recovery (MOLLI) for high-resolution T1 mapping of the heart. Magn Reson Med 2004;52:141–6. https://doi.org/10.1002/mrm.20110.

[13] Chow K, Flewitt JA, Green JD, Pagano JJ, Friedrich MG, Thompson RB. Saturation recovery single-shot acquisition (SASHA) for myocardial T1 mapping. Magn Reson Med 2014;71:2082–95. https://doi.org/10.1002/mrm.24878.

[14] Giri S, Chung YC, Merchant A, et al. T2 quantification for improved detection of myocardial edema. J Cardiovasc Magn Reson 2009;11(1):13. https://doi.org/10.1186/1532-429X-11-56.

[15] Sprinkart AM, Luetkens JA, Träber F, et al. Gradient Spin Echo (GraSE) imaging for fast myocardial T2 mapping. J Cardiovasc Magn Reson 2015;17(1):9. https://doi.org/10.1186/s12968-015-0127-z.

[16] Akçakaya M, Weingärtner S, Basha TA, Roujol S, Bellm S, Nezafat R. Joint myocardial T1 and T2 mapping using a combination of saturation recovery and T2-preparation. Magn Reson Med 2016;76:888–96. https://doi.org/10.1002/mrm.25975.

[17] Chow K, Hayes G, Flewitt JA, et al. Improved accuracy and precision with three-parameter simultaneous myocardial T1 and T2 mapping using multiparametric SASHA. Magn. Reson. Med. 2022;87:2775–91. https://doi.org/10.1002/mrm.29170.

[18] Santini F, Kawel-Boehm N, Greiser A, Bremerich J, Bieri O. Simultaneous T1 and T2 quantification of the myocardium using cardiac balanced-SSFP inversion recovery with interleaved sampling acquisition (CABIRIA). Magn Reson Med 2015;74:365–71. https://doi.org/10.1002/mrm.25402.

[19] Weingärtner S, Shenoy C, Rieger B, Schad LR, Schulz-Menger J, Akçakaya M. Temporally resolved parametric assessment of Z-magnetization recovery (TOPAZ): Dynamic myocardial T1mapping using a cine steady-state look-locker approach. Magn Reson Med 2018;79:2087–100. https://doi.org/10.1002/mrm.26887.

[20] Zhou R, Weller DS, Yang Y, et al. Dual-excitation flip-angle simultaneous cine and T1 mapping using spiral acquisition with respiratory and cardiac self-gating. Magn Reson Med 2021;86:82–96. https://doi.org/10.1002/mrm.28675.

[21] Becker KM, Schulz-Menger J, Schaeffter T, Kolbitsch C. Simultaneous high-resolution cardiac T1 mapping and cine imaging using model-based iterative image reconstruction. Magn Reson Med 2019;81:1080–91. https://doi.org/10.1002/mrm.27474.

[22] Wang X, Kohler F, Unterberg-Buchwald C, Lotz J, Frahm J, Uecker M. Model-based myocardial T1 mapping with sparsity constraints using single-shot inversion-recovery radial FLASH cardiovascular magnetic resonance. J Cardiovasc Magn Reson 2019;21:1–11. https://doi.org/10.1186/s12968-019-0570-3.

[23] Hermann I, Kellman P, Demirel OB, Akçakaya M, Schad LR, Weingärtner S. Free-breathing simultaneous T1, T2, and T2∗ quantification in the myocardium. Magn Reson Med 2021:1–15. https://doi.org/10.1002/mrm.28753.

[24] Guo R, Cai X, Kucukseymen S, Rodriguez J, Paskavitz A, Pierce P, Goddu B, Thompson RB, Nezafat R. Free-breathing simultaneous myocardial T1 and T2 mapping with whole left ventricle coverage. Magn Reson Med 2021;85(3):1308–21.

[25] Kvernby S, Warntjes M, Haraldsson H, Carlhall C-J, Engvall J, Ebbers T. Simultaneous three-dimensional myocardial T1 and T2 mapping in one breath hold with 3D-QALAS. J Cardiovasc Magn Reson 2014;16:102. https://doi.org/10.1002/mrm.21272.

[26] Kvernby S, Warntjes M, Engvall J, Carlhäll CJ, Ebbers T. Clinical feasibility of 3D-QALAS – Single breath-hold 3D myocardial T1- and T2-mapping. Magn Reson Imag 2017;38:13–20. https://doi.org/10.1016/j.mri.2016.12.014.

[27] Guo R, Chen Z, Herzka DA, Luo J, Ding H. A three-dimensional free-breathing sequence for simultaneous myocardial T1 and T2 mapping. Magn Reson Med 2019;81:1031–43. https://doi.org/10.1002/mrm.27466.

[28] Guo R, Si D, Chen Z, et al. Saturation-recovery and Variable-flip-Angle–based three-dimensional free-breathing cardiovascular magnetic resonance T1 mapping at 3 T. NMR Biomed 2022:1–12. https://doi.org/10.1002/nbm.4755.

[29] Milotta G, Bustin A, Jaubert O, Neji R, Prieto C, Botnar RM. 3D whole-heart isotropic-resolution motion-compensated joint T1/T2 mapping and water/fat imaging. Magn Reson Med 2020;84:3009–26. https://doi.org/10.1002/mrm.28330.

[30] Qi H, Bustin A, Cruz G, et al. Free-running simultaneous myocardial T1/T2 mapping and cine imaging with 3D whole-heart coverage and isotropic spatial resolution. Magn Reson Imag 2019;63:159–69. https://doi.org/10.1016/j.mri.2019.08.008.

[31] Ma D, Gulani V, Seiberlich N, Liu K, Sunshine JL, Duerk JL, Griswold MA. Magnetic resonance fingerprinting. Mar 14 Nature 2013;495(7440):187–92. https://doi.org/10.1038/nature11971. PMID: 23486058; PMCID: PMC3602925.

[32] Zhao B, Haldar JP, Liao C, et al. Optimal Experiment Design for Magnetic Resonance Fingerprinting: Cramér-Rao Bound Meets Spin Dynamics. 1 IEEE Trans Med Imag2018. https://doi.org/10.1109/TMI.2018.2873704.

[33] Asslander J, Novikov DS, Lattanzi R, Sodickson DK, Cloos MA. Hybrid-state free precession in nuclear magnetic resonance. Commun Phys 2019;2:1–73. https://doi.org/10.1103/PhysRev.112.1693.

[34] Leitão D, Teixeira RPAG, Price A, Uus A, Hajnal JV, Malik SJ. Efficiency analysis for quantitative MRI of T1 and T2 relaxometry methods. Phys Med Biol 2021:66. https://doi.org/10.1088/1361-6560/ac101f.

[35] Hamilton JI, Jiang Y, Chen Y, Ma D, Lo WC, Griswold M, Seiberlich N. MR fingerprinting for rapid quantification of myocardial T1, T2, and proton spin density. Magn Reson Med 2017;77(4):1446–58. https://doi.org/10.1002/mrm.26216. Epub 2016 Apr 1. PMID: 27038043; PMCID: PMC5045735.

[36] Hamilton JI, Jiang Y, Ma D, et al. Investigating and reducing the effects of confounding factors for robust T1 and T2 mapping with cardiac MR fingerprinting. Magn Reson Imag 2018;53:40–51. https://doi.org/10.1016/j.mri.2018.06.018.

[37] Liu Y, Hamilton J, Rajagopalan S, Seiberlich N. Cardiac Magnetic Resonance Fingerprinting: Technical Overview and Initial Results. JACC Cardiovasc Imag 2018;11:1837–53. https://doi.org/10.1016/j.jcmg.2018.08.028.

[38] Cruz G, Jaubert O, Botnar RM, Prieto C. Cardiac magnetic resonance fingerprinting: technical developments and initial clinical validation. Curr Cardiol Rep 2019:21. https://doi.org/10.1007/s11886-019-1181-1.

[39] Eck BL, Flamm SD, Kwon DH, Tang WHW, Vasquez CP, Seiberlich N. Cardiac magnetic resonance fingerprinting: trends in technical development and potential clinical applications. Prog Nucl Magn Reson Spectrosc 2021;122:11–22. https://doi.org/10.1016/j.pnmrs.2020.10.001.

[40] Jaubert O, Cruz G, Bustin A, et al. Water–fat Dixon cardiac magnetic resonance fingerprinting. Magn Reson Med 2019:mrm.28070. https://doi.org/10.1002/mrm.28070.

[41] Liu Y, Hamilton J, Eck B, Griswold M, Seiberlich N. Myocardial T1 and T2 quantification and water–fat separation using cardiac MR fingerprinting with rosette trajectories at 3T and 1.5T. Magn Reson Med 2021;85:103–19. https://doi.org/10.1002/mrm.28404.

[42] Hamilton JI, Ma D, Chen Y, Seiberlich N. Simultaneous multislice cardiac magnetic resonance fingerprinting using low rank reconstruction. NMR Biomed 2019:1–16. https://doi.org/10.1002/nbm.4041.

[43] Hamilton JI, Pahwa S, Adedigba J, et al. Simultaneous mapping of T1 and T2 using cardiac magnetic resonance fingerprinting in a cohort of healthy. Subjects at 1. 5T. J. Magn Reson Imag 2020;52:1044–52. https://doi.org/10.1002/jmri.27155.

[44] Cavallo AU, Liu Y, Patterson A, et al. CMR Fingerprinting for Myocardial T1, T2, and ECV Quantification in Patients With Nonischemic Cardiomyopathy. JACC Cardiovasc. Imaging 2019;12:1584–5. https://doi.org/10.1016/j.jcmg.2019.01.034.

[45] Jaubert O, Cruz G, Bustin A, et al. T1, T2, and fat fraction cardiac mr fingerprinting: preliminary clinical evaluation. J Magn Reson Imag 2020. https://doi.org/10.1002/jmri.27415.

[46] Liu, Y., Hamilton, J., Jiang, Y. and Seiberlich, N., Cardiac MRF Using Rosette Trajectories for Simultaneous Myocardial T1, T2, and Proton Density Fat Fraction Mapping. Frontiers in Cardiovascular Medicine, p.977603, in press.

[47] Lima da Cruz GJ, Velasco C, Lavin B, Jaubert O, Botnar RM, Prieto C. Myocardial T1, T2, T2*, and fat fraction quantification via low-rank motion-corrected cardiac MR fingerprinting. Magn Reson Med 2022;87:2757–74. https://doi.org/10.1002/mrm.29171.

[48] Velasco C, Cruz G, Lavin B, et al. Simultaneous T1, T2, and T1ρ cardiac magnetic resonance fingerprinting for contrast agent–free myocardial tissue characterization. Magn Reson Med 2022;87:1992–2002. https://doi.org/10.1002/mrm.29091.

[49] Hamilton JI, Jiang Y, Eck B, Griswold M, Seiberlich N. Cardiac cine magnetic resonance fingerprinting for combined ejection fraction, T1 and T2 quantification. NMR Biomed 2020:1–17. https://doi.org/10.1002/nbm.4323.

[50] Jaubert O, Cruz G, Bustin A, et al. Free-running cardiac magnetic resonance fingerprinting: Joint T1/T2 map and Cine imaging. Magn Reson Imag 2020;68:173–82. https://doi.org/10.1016/j.mri.2020.02.005.

[51] Cruz G, Jaubert O, Qi H, et al. 3D free-breathing cardiac magnetic resonance fingerprinting. NMR Biomed 2020:1–16. https://doi.org/10.1002/nbm.4370.

[52] Cruz G, Qi H, Jaubert O, et al. Generalized low-rank nonrigid motion-corrected reconstruction for MR fingerprinting. Magn Reson Med 2022;87:746–63. https://doi.org/10.1002/mrm.29027.

[53] Velasco C, Fletcher TJ, Botnar RM, Prieto C. Artificial intelligence in cardiac magnetic resonance fingerprinting. Front Cardiovasc Med 2022;9:1009131. https://doi.org/10.3389/fcvm.2022.1009131. PMID: 36204566; PMCID: PMC9530662.

[54] Hamilton JI, Currey D, Rajagopalan S, Seiberlich N. Deep learning reconstruction for cardiac magnetic resonance fingerprinting T1 and T2 mapping. Magn Reson Med 2021;85:2127–35. https://doi.org/10.1002/mrm.28568.

[55] Cohen O, Zhu B, Rosen MS. MR fingerprinting Deep RecOnstruction NEtwork (DRONE). Magn Reson Med 2018;80:885–94. (doi:10.1002/mrm.27198).

[56] Hamilton JI. A Self-Supervised Deep Learning Reconstruction for Shortening the Breathhold and Acquisition Window in Cardiac Magnetic Resonance Fingerprinting. Front Cardiovasc Med 2022;9:928546. https://doi.org/10.3389/fcvm.2022.928546. PMID: 35811730; PMCID: PMC9260051.

[57] Christodoulou AG, Shaw JL, Nguyen C, et al. Magnetic resonance multitasking for motion-resolved quantitative cardiovascular imaging. Nat Biomed Eng 2018;2:215–26. https://doi.org/10.1038/s41551-018-0217-y.

[58] Serry FM, Ma S, Mao X, et al. Dual flip-angle IR-FLASH with spin history mapping for B1 + corrected T1 mapping: Application to T1 cardiovascular magnetic resonance multitasking. Magn Reson Med 2021:1–10. https://doi.org/10.1002/mrm.28935.

[59] Mao X, Lee H-L, Hu Z, et al. Simultaneous Multi-Slice Cardiac MR Multitasking for Motion-Resolved, Non-ECG, Free-Breathing T1–T2 Mapping. Front Cardiovasc Med 2022;9:1–13. https://doi.org/10.3389/fcvm.2022.833257.

[60] Shaw JL, Yang Q, Zhou Z, et al. Free-breathing, non-ECG, continuous myocardial T1 mapping with cardiovascular magnetic resonance multitasking. Magn Reson Med 2019;81:2450–63. https://doi.org/10.1002/mrm.27574.

[61] Han P, Zhang R, Wagner S, Xie Y, Cingolani E, Marban E, Christodoulou AG, Li D. Electrocardiogram-less, free-breathing myocardial extracellular volume fraction mapping in small animals at high heart rates using motion-resolved cardiovascular magnetic resonance multitasking: a feasibility study in a heart failure with preserved ejection fraction rat model. J Cardiovasc Magn Reson 2021;23(1):8.

[62] Nguyen CT, Christodoulou AG, Coll-Font J, et al. Free-breathing diffusion tensor MRI of the whole left ventricle using second-order motion compensation and multitasking respiratory motion correction. Magn Reson Med 2021;85:2634–48. https://doi.org/10.1002/mrm.28611.

[63] Cao T, Wang N, Kwan AC, et al. Free-breathing, non-ECG, simultaneous myocardial T1, T2, T2*, and fat-fraction mapping with motion-resolved cardiovascular MR multitasking. Magn Reson Med 2022:1–16. https://doi.org/10.1002/mrm.29351.

[64] Hu Z, Xiao J, Mao X, Xie Y, Kwan AC, Song SS, Fong MW, Wilcox AG, Li D, Christodoulou AG, Fan Z. MR Multitasking-based multi-dimensional assessment of cardiovascular system (MT-MACS) with extended spatial coverage and water-fat separation. Magn Reson Med 2023;89:1496–505. PMID: 36336794.

[65] Mao X, Lee H-L, Kwan AC, Cao T, Han F, Xie Y, Li D, Christodoulou A. 3D joint reconstruction of non-contrast and contrast-enhanced CMR multitasking. ISMRM. 2022. p. 274.

[66] Wang N, Cao T, Han F, Xie Y, Zhong X, Ma S, Fan Z, Han H, Bi X, Noureddin M, Deshpande V, Christodoulou AG, Li D. Free-breathing multitasking multi-echo MRI for whole-liver water-specific T1, proton density fat fraction, and R2* quantification. Magn Reson Med 2022;87:120–37.

[67] Coniglio A, Di Renzi P, Vilches Freixas G, Della Longa G, Santarelli A, Capparella R, Nardiello B, Loiudice C, Bianchi S, D'Arienzo M, Begnozzi L. Multiple 3D inversion recovery imaging for volume T1 mapping of the heart. (Jan). Magn Reson Med 2013;69(1):163–70. https://doi.org/10.1002/mrm.24248.

[68] van Heeswijk RB, Piccini D, Feliciano H, Hullin R, Schwitter J, Stuber M. Self-navigated isotropic three-dimensional cardiac T2 mapping. Magn Reson Med 2015;73(4):1549–54. https://doi.org/10.1002/mrm.25258. Epub 2014 May 8. PMID: 24809849.

[69] Kamesh Iyer S, Moon B, Hwuang E, Han Y, Solomon M, Litt H, Witschey WR. Accelerated free-breathing 3D T1ρ cardiovascular magnetic resonance using multicoil compressed sensing. J Cardiovasc Magn Reson 2019;21(1):5. https://doi.org/10.1186/s12968-018-0507-2. PMID: 30626437; PMCID: PMC6327532.

[70] Leiner T, Rueckert D, Suinesiaputra A, et al. Machine learning in cardiovascular magnetic resonance: basic concepts and applications. J Cardiovasc Magn Reson 2019;21:61.

[71] Davies RH, et al. Precision measurement of cardiac structure and function in cardiovascular magnetic resonance using machine learning. J Cardiovasc Magn Reson 2022;24(1):16.

[72] Xue H, et al. Automated In-Line Artificial Intelligence Measured Global Longitudinal Shortening and Mitral Annular Plane Systolic Excursion: Reproducibility and Prognostic Significance. J Am Heart Assoc 2022;11(4):e023849.

[73] Zhang Q, Burrage MK, Lukaschuk E, Shanmuganathan M, Popescu IA, Nikolaidou C, Mills R, Werys K, Hann E, Barutcu A, Polat SD. Toward replacing late gadolinium enhancement with artificial intelligence virtual native enhancement for gadolinium-free cardiovascular magnetic resonance tissue characterization in hypertrophic cardiomyopathy. Circulation 2021;144(8):589–99.

[74] Chen, Y., Shaw, J.L., Xie, Y., Li, D. and Christodoulou, A.G., 2019, October. Deep learning within a priori temporal feature spaces for large-scale dynamic MR image reconstruction: Application to 5-D cardiac MR Multitasking. In International Conference on Medical Image Computing and Computer-Assisted Intervention (pp. 495–504).

[75] Chen, Z., Chen, Y., Xie, Y., Li, D. and Christodoulou, A.G., 2022, March. Data-Consistent non-Cartesian deep subspace learning for efficient dynamic MR image reconstruction. In IEEE International Symposium on Biomedical Imaging (ISBI).

[76] Zou Q, Priya S, Nagpal P, Jacob M. Joint cardiac T 1 mapping and cardiac cine using manifold modeling. Bioengineering 2023;10(3):345.

[77] Yaman B, Hosseini SA, Moeller S, Ellermann J, Uğurbil K, Akçakaya M. Self-supervised learning of physics-guided reconstruction neural networks without fully sampled reference data. Magn Reson Med 2020;84(6):3172–91.

[78] Alex Fyrdahl, Nicole Seiberlich, Jesse Hamilton. Online FIRE Reconstruction of Cardiac MRF T1, T2 and ECV maps with Neural Network Dictionary Generation and Low-Rank Subspace Reconstruction. Proc. Annual Meeting of the ISMRM, 2022.

[79] Axel L, Phan TS, Metaxas DN. Visualization and analysis of multidimensional cardiovascular magnetic resonance imaging: challenges and opportunities. Front Cardiovasc Med 2022;9.

[80] Piekarski E, Chitiboi T, Ramb R, Feng L, Axel L. Use of self-gated radial cardiovascular magnetic resonance to detect and classify arrhythmias (atrial fibrillation and premature ventricular contraction). J Cardiovasc Magn Reson 2017;18(1):83.

[81] Ma L, Yerly J, Di Sopra L, Piccini D, Lee J, DiCarlo A, Passman R, Greenland P, Kim D, Stuber M, Markl M. Using 5D flow MRI to decode the effects of rhythm on left atrial 3D flow dynamics in patients with atrial fibrillation. Magn Reson Med 2021;85(6):3125–39.

[82] Chitiboi T, Ramb R, Feng L, Piekarski E, Tautz L, Hennemuth A, Axel L. Multi-cycle reconstruction of cardiac MRI for the analysis of inter-ventricular septum motion during free breathing. Funct Imaging Model Heart 2017;10263:63–72. https://doi.org/10.1007/978-3-319-59448-4_7. Epub 2017 May 23. PMID: 30498813; PMCID: PMC6258012.

[83] Cohen O, Otazo R. Global deep learning optimization of chemical exchange saturation transfer magnetic resonance fingerprinting acquisition schedule. NMR Biomed 2023:e4954. https://doi.org/10.1002/nbm.4954. Epub ahead of print. PMID: 37070221.

[84] Cohen O, Yu VY, Tringale KR, Young RJ, Perlman O, Farrar CT, Otazo R. CEST MR fingerprinting (CEST-MRF) for brain tumor quantification using EPI readout and deep learning reconstruction. Magn Reson Med 2023;89(1):233–49. https://doi.org/10.1002/mrm.29448. Epub 2022 Sep 21. PMID: 36128888; PMCID: PMC9617776.

[85] Singh M, Jiang S, Li Y, van Zijl P, Zhou J, Heo HY. Bloch simulator-driven deep recurrent neural network for magnetization transfer contrast MR fingerprinting and CEST imaging. Magn Reson Med 2023. https://doi.org/10.1002/mrm.29748. Epub ahead of print. PMID: 37317675.

[86] Fotaki A, Puyol-Antón E, Chiribiri A, Botnar R, Pushparajah K, Prieto C. Artificial intelligence in cardiac MRI: is clinical adoption forthcoming? Front Cardiovasc Med 2022;8:818765. https://doi.org/10.3389/fcvm.2021.818765. PMID: 35083303; PMCID: PMC8785419.